A Quasi-Steady Evaluation of Submarine Rising Stability: The Stability Limit

George D. Watt
watt@drea.dnd.ca
Defence Research Establishment Atlantic
PO Box 1012, Dartmouth NS B2Y 3Z7, Canada

Abstract

When submarines blow ballast to surface from depth in an emergency, they can experience a roll instability if they ascend with large flow incidence angles. It is shown that an instability is caused by the destabilizing hydrodynamic rolling moment on the sail (which points upwards into the onset crossflow) overcoming the static righting moment (the center of gravity is below the center of buoyancy) as the boat is accelerated upwards by buoyancy. The former increases with velocity squared while the latter is constant. Conventional first order rolling moment models are shown to underpredict the nonlinear hydrodynamic rolling moment, especially at high incidence angles. However, properly modelling the quasi-steady hydrodynamics still does not fully explain the early onset of the roll instability.

Nomenclature

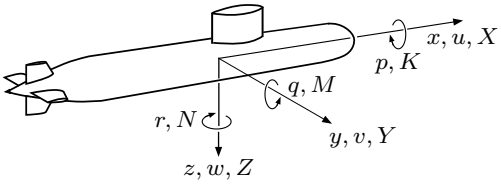

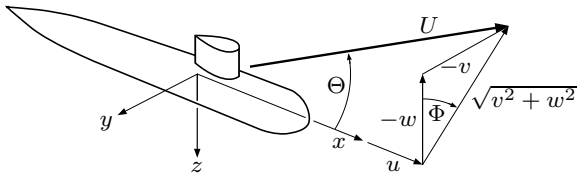

$\mathrm{B} = \rho \mathrm{Vg}$	Buoyancy; defined by the external hydrodynamic envelope.
$\overline{BG}$	Height of center of buoyancy above center of gravity.
d	Maximum hull diameter.
g	Gravitational constant.
K, M, N	Body axis moments.
K', M', N'	Moments nondimensionalized using $\rho U^2 \ell^3/2$.
ℓ	Overall length of submarine.
p, q, r	Body axis angular velocities.
$R_{\mathrm{HSSD(T)}}$	Stability derivative with or without the tailplanes.
R	Reynolds number, based on submarine length ℓ.
t	Time.
u, v, w	Body axis velocities.
$U = \sqrt{u^2 + v^2 + w^2}$	Boat speed.
V	Volume of external hydrodynamic envelope.
W	Weight; changes as ballast tanks are blown or flooded.

Paper presented at the RTO AVT Symposium on "Advanced Flow Management: Part A – Vortex Flows and High Angle of Attack for Military Vehicles", held in Loen, Norway, 7-11 May 2001, and published in RTO-MP-069(I).

Report Documentation Page

Form Approved
OMB No. 0704-0188

1. REPORT DATE	2. REPORT TYPE	3. DATES COVERED
00 MAR 2003	**N/A**	**-**

4. TITLE AND SUBTITLE	5a. CONTRACT NUMBER
A Quasi-Steady Evaluation of Submarine Rising Stability: The Stability Limit	5b. GRANT NUMBER
	5c. PROGRAM ELEMENT NUMBER
6. AUTHOR(S)	5d. PROJECT NUMBER
	5e. TASK NUMBER
	5f. WORK UNIT NUMBER
7. PERFORMING ORGANIZATION NAME(S) AND ADDRESS(ES) **NATO Research and Technology Organisation BP 25, 7 Rue Ancelle, F-92201 Neuilly-Sue-Seine Cedex, France**	8. PERFORMING ORGANIZATION REPORT NUMBER
9. SPONSORING/MONITORING AGENCY NAME(S) AND ADDRESS(ES)	10. SPONSOR/MONITOR'S ACRONYM(S)
	11. SPONSOR/MONITOR'S REPORT NUMBER(S)

12. DISTRIBUTION/AVAILABILITY STATEMENT
Approved for public release, distribution unlimited

13. SUPPLEMENTARY NOTES
Also see: ADM001490, Presented at RTO Applied Vehicle Technology Panel (AVT) Symposium held inLeon, Norway on 7-11 May 2001, The original document contains color images.

14. ABSTRACT

15. SUBJECT TERMS

16. SECURITY CLASSIFICATION OF:			17. LIMITATION OF ABSTRACT	18. NUMBER OF PAGES	19a. NAME OF RESPONSIBLE PERSON
a. REPORT	b. ABSTRACT	c. THIS PAGE			
unclassified	**unclassified**	**unclassified**	**UU**	**18**	

x, y, z	Submarine body fixed axes, with origin on the hull centerline.
X, Y, Z	Body axis forces.
X', Y', Z'	Forces nondimensionalized using $\rho U^2 \ell^2/2$.
θ, ϕ	Pitch and roll Euler angles giving boat orientation.
$\Theta = \tan^{-1}(\sqrt{v^2+w^2}/u)$	Flow incidence angle; $\Theta \geq 0$ always.
ρ	Fluid density.
τ_T	Time for the flow to convect from the sail to the tail.
$\Phi = \tan^{-1}(-v/-w)$	Flow orientation angle; $\Phi = 0$ when the sail points in the direction of the transverse velocity component of the boat.

The following relations are useful:

$$u = U\cos\Theta\,, \quad v = -U\sin\Theta\sin\Phi\,, \quad w = -U\sin\Theta\cos\Phi\,, \quad \sqrt{v^2+w^2} = U\sin\Theta\,.$$

1 Introduction

1.1 Background

Safety is a very important consideration in the design and operation of submarines. To reduce risk while at depth, submarines are usually equipped with emergency systems designed to rapidly blow the ballast tanks allowing a boat to surface quickly. This results in the boat rising rapidly at incidence with its sail pointing upwards into the crossflow. This destabilizing flow is countered by the static stability of the boat (the center of gravity is below the center of buoyancy). Complicating the emergency rise are:

- unsteady forces and possibly asymmetric vortex shedding at very high flow incidence,
- the escape of expanding ballast tank air as the depth decreases, and
- the sudden, temporary loss of static stability at the surface caused by slow-to-drain flood water in the sail and deckcasing.

Rising at high incidence can result in unpredictable motions, including large roll oscillations. Wichers Schreur [1] documents such motions for buoyant circular cylinders rising vertically (no forward speed) with and without simulated deck and appendage geometry, albeit at low Reynolds numbers. He found that bare cylinders experienced unpredictable sway and yaw motions, attributed to unsteady vortex shedding in the wake. When vertical vanes were attached atop the cylinder, roll amplitudes ranging from 30 to 150 degrees were obtained.

Binion and Stanewsky [2] survey the literature on high incidence missile aerodynamics. They consider Reynolds numbers just high enough to be applicable to rising submarines. They note the flow characteristics are a strong function of both incidence and Reynolds number. For missile bodies (sharp noses, truncated tails) with length to diameter ratios similar to submarines, the wake is steady with symmetric separation vortices at incidence angles up to 20 or 30 degrees, steady with asymmetric vortices up to 60 or 70 degrees, and unsteady beyond that. The steady asymmetric vortex wake is attributed to unavoidable, minor geometrical asymmetries in the nose. An asymmetric wake induces side force which would roll a submarine as the sail resists the resulting lateral movement of the hull.

In light of the above information, it is desirable for a submarine to rise at incidence angles less than 20 to 30 degrees, so that its motions are at least predictable. Figure 1 shows an example of a limited and controlled emergency rise. The maneuver is limited because the ballast blowing time is limited and not all ballast tanks are blown. It is controlled because the forward speed and pitch angle of the boat are used to reduce flow incidence.

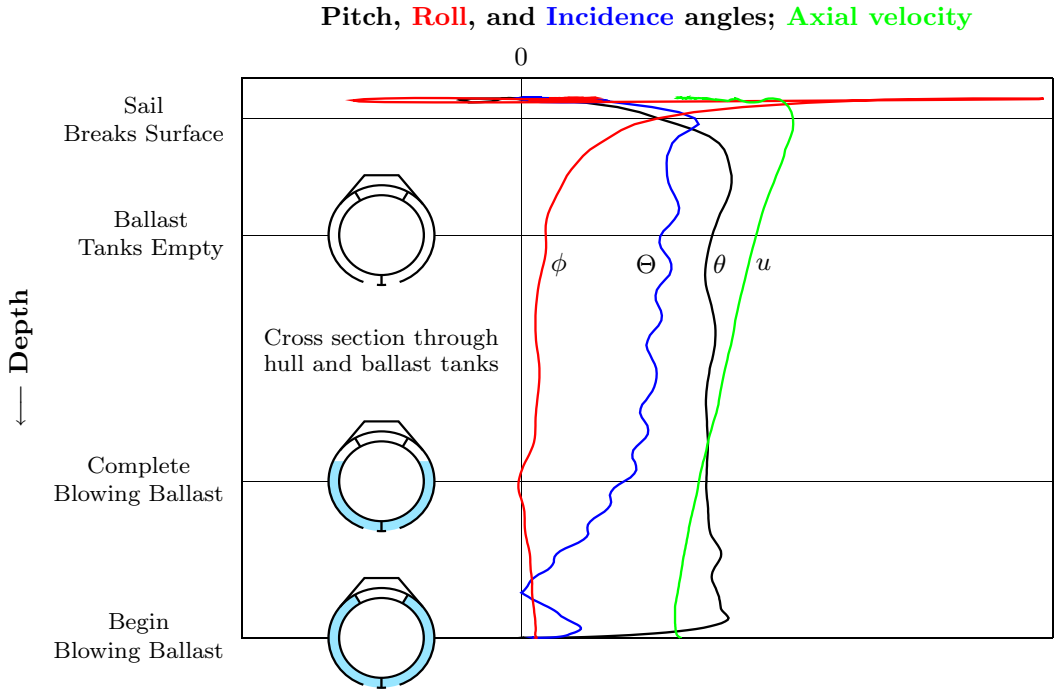

Figure 1 *A limited and controlled emergency rise from depth.*

The maneuver in Figure 1 starts when ballast tank blowing begins at depth. Forward speed is such that the response to sternplane control is good and the desired pitch-up attitude (θ) is immediately achieved. As the blowing progresses, the rising velocity and therefore flow incidence (Θ) increase. The rate of increase of incidence tapers off when the blow is complete, but continues as the air expands in the tanks increasing the buoyancy. The increase in incidence is also curtailed by the steadily increasing forward speed of the boat, resulting from its pitch-up attitude.

Roll angle (ϕ) is small through most of the rise, until just after the ballast tanks empty. While the tanks are emptying, the center of gravity is lowered temporarily increasing static stability, extra stability that is lost just as the tanks empty and the roll excursion begins. Also at this time, the continually expanding air in the tanks begins escaping around the boat, possibly about the sail. When the submarine rises above the surface, it temporarily loses static stability until water has drained from the sail and deck casing. A large surface roll angle is attained before enough flood water has drained to restore stability. The boat then rolls back to, and undergoes a damped oscillation about, zero roll angle.

Despite the care taken conducting this maneuver, an uncomfortably large roll angle still occurred on the surface. The temporary hydrostatic instability a submarine experiences when surfacing is well understood and normally not a problem; however, the instability is aggravated by a large emergence roll angle which, in the above maneuver, is the result of a submerged instability that is not understood [3,4].

Booth [5,6] carries out a classical stability analysis of a rising, buoyant submarine. The analysis is linearized in the horizontal plane motions v, p, r for arbitrarily large values of the vertical plane crossflow velocity w. This analysis is late at predicting the roll instability; that is, it puts the stability limit at velocity and flow incidence angles about twice as high as occur in Figure 1.

1.2 Current Work

The first step in trying to understand the submerged instability is to examine the limitations of the standard hydrodynamics models. A well known version of these models are the Gertler and Hagen [7] six degrees-of-freedom equations of motion for a maneuvering submarine. Feldman [8] updates these equations and explains the changes in [9] and [10]. These equations are widely used and provide realistic simulations when motions are not extreme. The standard rolling moment equation is discussed in §2.

The standard hydrodynamics models are based on towing tank data primarily acquired at incidence angles up to 18 degrees in only the horizontal and vertical planes (yaw and pitch tests). To assess their limitations, preliminary overall force measurements were made at incidence angles up to 90 degrees at several flow orientation angles. This work is summarized in §3. It confirms the unsteady, difficult-to-predict nature of very high incidence flows and shows where radical changes in the flow occur. It also provides perspective, showing where the standard models break down.

Subsequent, more accurate, high Reynolds number experiments at up to 30 degrees incidence were carried out with roll angle as the primary independent variable. These results are presented in §4 and are used in §5 to analyze the underwater roll instability. This analysis is relatively simple and provides analytical expressions for predicting instability. It accounts for nonlinearity in the total crossflow velocity ($\sqrt{v^2+w^2}$) and is based on data measured from near vertical ascent flow orientations. It gives earlier predictions of the instability than does Booth's approach but still not early enough to satisfactorily explain the Figure 1 underwater roll excursion.

2 The Standard Rolling Moment Equation

The standard equations of motion model the hydrodynamic forces with up to second order terms in the state variables. In the Feldman [8] version of the equations, strip theory is used to account for axial variations in crossflow drag and the strength of vorticity trailing from the sail. Coefficients in the models are generally set using information from only the 0 to 18 degree incidence range. This maximizes model accuracy in the range where most maneuvers of interest occur, but does not provide reliable modelling at high incidence. Also, the models generally use simple sinusoidal interpolation between yaw and pitch test data to predict combined horizontal and vertical plane motions.

A slightly simplified version of the Feldman rolling moment equation of motion is:

$$
\begin{aligned}
&I_{xx}\dot{p} + \big(I_{zz} - I_{yy}\big)qr - \big(\dot{r} + pq\big)I_{zx} + \big(r^2 - q^2\big)I_{yz} + \big(pr - \dot{q}\big)I_{xy} \\
&\quad + m\big[y_G(\dot{w} - uq + vp) - z_G(\dot{v} - wp + ur)\big] \\
&\qquad = \frac{\rho}{2}\ell^5\big[K'_{\dot{p}}\dot{p} + K'_{\dot{r}}\dot{r} + K'_{qr}qr + K'_{p|p|}p|p|\big] \\
&\qquad\quad + \frac{\rho}{2}\ell^4\big[K'_{p}up + K'_{r}ur + K'_{\dot{v}}\dot{v} + K'_{wp}wp\big] \\
&\qquad\quad + \frac{\rho}{2}\ell^3\Big[K'_{*}u^2 + K'_{vR}uv + K'_{i}uv_{FW}(t-\tau_T) + f(\delta_r) \\
&\qquad\qquad\qquad + (u^2 + v_T^2 + w_T^2)\Theta_T^2(K'_{4T}\sin 4\Phi_T + K'_{8T}\sin 8\Phi_T)\Big] \\
&\qquad\quad + \frac{\rho}{2}\ell^2\frac{\bar{z}}{\ell}\overline{C}_L\int_{\text{afterbody}} w(x)\,\bar{v}_{FW}\big(t-\tau(x)\big)\,dx \\
&\qquad\quad + \big(y_G W - y_B B\big)\cos\theta\cos\phi - \big(z_G W - z_B B\big)\cos\theta\sin\phi - Q_p
\end{aligned}
\tag{1}
$$

It is understood that this generic formulation should be adapted, as required, to each application. The equation is a body axes formulation of Newton's second law for moments and is derived in its basic form by Abkowitz [11]. The LHS consists of the submarine mass m and moments of inertia I multiplying various acceleration terms.

The RHS is the sum of all rolling moments acting on the submarine. It contains several constant K' coefficients that are determined for each application. The $\dot{p}, \dot{r}, \dot{v}$ terms are added mass moments and the qr and wp terms are suggested by a potential flow analysis primarily aimed at estimating added mass [12,13]. The p and $p|p|$ terms are roll damping and crossflow drag terms. The $K'_* u^2$ term accounts for any trim anomalies and is usually zero. The last line of (1) gives the static roll stability as the resolution of weight W and buoyancy B acting through the centers of gravity (subscript G) and buoyancy (subscript B); Q_p is the torque induced by the propulsion system. The horizontal plane rotation r and rudder deflection δ_r are assumed to be zero in the current problem.

The rolling moment on a submarine with an axisymmetric hull consists of two main parts: moment on the sail and on the tail. The latter is primarily generated from trailing vorticity from the sail interacting with the tail appendages. This interaction is proportional to the strength of the trailing vorticity opposite the tail, which is proportional to the crossflow at the sail v_{FW} (fairwater is another name for sail) at $t = \tau_T \approx u(x_{\text{sail}} - x_{\text{tail}})$ seconds ago. In a static experiment the sail crossflow does not change with time, so $K'_{vR} uv + K'_i uv_{FW}(t - \tau_T) = K'_v uv$. For the general unsteady case, K'_i is that part of K'_v giving the tail induced moment and K'_{vR} is the remainder.

The third from last line in (1) models asymmetric lift on the tailplanes caused by the wake shadow from the hull in the local crossflow having incidence Θ_T and flow orientation Φ_T (subscript T for tail). This is one term which does use high order Φ interpolation, but it is shown to be insignificant for the current problem.

The integral in (1) gives the lateral component of 'out-of-plane' lift acting over the afterbody as a result of interaction of the local crossflow with afterbody bound vorticity from the sail — the Magnus effect. This lateral force acts at the vertical centerline $z = \bar{z}$ to induce a rolling moment. $\bar{z} = 0$ for an axisymmetric hull and it is still quite small when a small deck is added, so this term is negligible in the current problem.

The main limitation in (1) is that it does not provide enough flexibility to model the moment at all roll orientations at the moderate to high incidence angles of interest in the rising stability problem. Further, adding degrees of freedom to this state velocity formulation is not straightforward. The problem is addressed in §4 by reformulating the hydrodynamic moment as double quasi-Fourier series in the incidence and flow orientation angles Θ and Φ. These angles have easily understood physical meaning at all flow orientations, unlike the more conventional angles of attack α and drift β which are intuitively clear only for motion in the vertical or horizontal planes.

3 Blowdown Tunnel Very High Incidence Data

To obtain overall force characteristics over a wide range of incidence and flow orientation angles, a 'quick and dirty' test program was carried out in the National Research Council's Institute for Aerospace Research (IAR) 1.5 m variable density blowdown wind tunnel in Ottawa. A sting mounted generic diesel-electric submarine shape was tested at Reynolds numbers around 10 million. Corrections for sting tare and interference effects were not made. The rolling moment measurements from these tests are presented in Figure 2.

Figure 2b presents rolling moment measurements from eight separate runs, most of which are at $\mathbf{R} = 10$ million. These are horizontal plane yaw tests. The inherent error in these data is relatively high, as seen by its spread at low Θ angles (where repeatability should be good) and its offset from the origin.

Model vibration during the $\Phi = 90$ degree incidence sweeps became noticeable at about $\Theta = 22$ to 24 degrees when the sail partially stalled. The vibration increased dramatically at about 50 degrees incidence where the balance was dynamically overloaded during the single $\mathbf{R} = 12$ million run, necessitating termination of the sweep. Three $\mathbf{R} = 10$ million runs were also terminated due to balance overload, between incidence angles of 57 and 77 degrees. This vibration is consistent with the flow structures expected at these incidence angles.

The variation in the Figure 2b measurements increases substantially beyond sail stall. The stall angle and the degree of stall appear to be dependent on both Reynolds number and ambient vibration. This should be kept in mind in any attempt to analyze motions in the post-stall regime using quasi-steady theory.

Although rising stability is a phenomenon associated with low Φ angles, the $\Phi = 90$ degree flow characteristics are relevant because they completely determine how the standard equation models rolling moment near $\Phi = 0$. Vertical plane tests provide no input since $K = 0$ at $\Phi = 0$. In a steady uniform flow over a submarine with an axisymmetric hull, the hydrodynamic moment in (1) reduces to:

$$K' = K'_v \frac{uv}{U^2} = -K'_v \sin\Theta \cos\Theta \sin\Phi \tag{2}$$

assuming the hull wake shadow does not contribute to the rolling moment at the tail. The value for the constant K'_v is usually set by a least squares fit of (2) to $\Theta = 0$ to 18 degree, $\Phi = 90$ degree data, as has been done in Figure 2b (the fit is shown as a solid black line and is extrapolated as a dashed line out to $\Theta = 90$ degrees). This ensures that a general purpose model properly simulates roll during common horizontal plane turning maneuvers, which occur at or about $\Phi = 90$ degrees.

Figure 2c shows the rolling moment incidence sweep data at Φ angles more applicable to the rising stability problem. Also shown is the fit (2), again using dashed lines where it is extrapolated beyond its region of applicability.

Figure 2d shows cross-plots of the incidence sweep data. This presentation is of greatest interest to the current problem since the underwater roll excursion in Figure 1 takes place at approximately constant incidence. And the roll stability at constant incidence is determined by the slopes of the constant Θ curves at $\Phi = 0$ in this figure.

The assumption in (2) that the moment reduces as $\sin\Phi$ does surprisingly well at low incidence angles in Figure 2d. However, $\partial K/\partial\Phi$ at $\Phi = 0$ is not well modelled for $\Theta \geq 16$ degrees, potentially important operating states in an emergency rise. More degrees of freedom in Φ are required in (2) to correct this situation while still providing a good model at $\Phi = 90$ degrees.

Similarly, since the curvature of the fit (2) is incorrect in the pre-stall regime in Figure 2b, more degrees-of-freedom in Θ are also required. These problems are corrected in the next section with the addition to K' of terms similar to $v\sqrt{v^2 + w^2} \propto \sin^2\Theta \sin\Phi$ and $vw \propto \sin^2\Theta \sin 2\Phi$, terms also used by Gertler and Hagen [7].

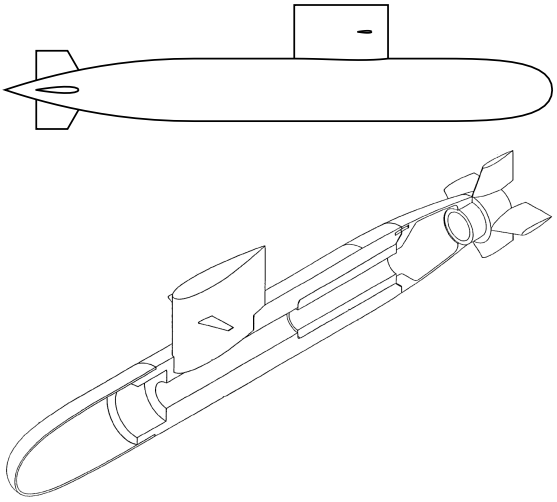

a) *The generic test shape with axisymmetric hull (ℓ/d = 8.75), symmetric tail, sailplanes, and a sail size typical of diesel-electric submarines. The 37 cm long blowdown tunnel test model (bottom) was sting mounted on an internal strain gauge balance.*

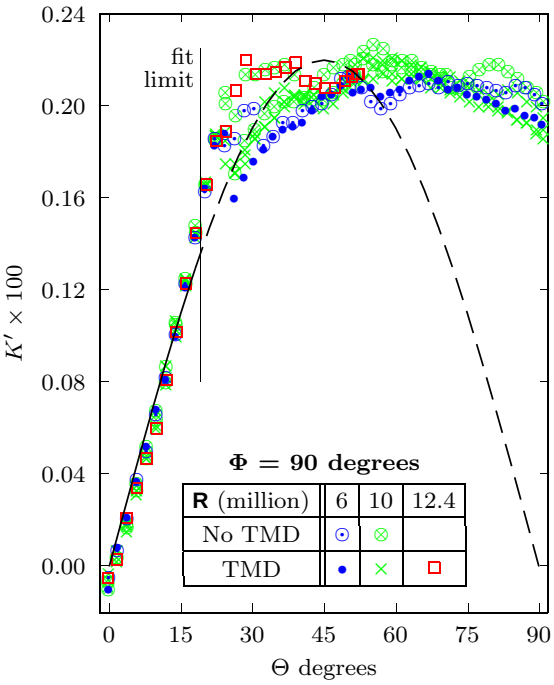

b) *Rolling moment versus incidence angle in the horizontal plane.*

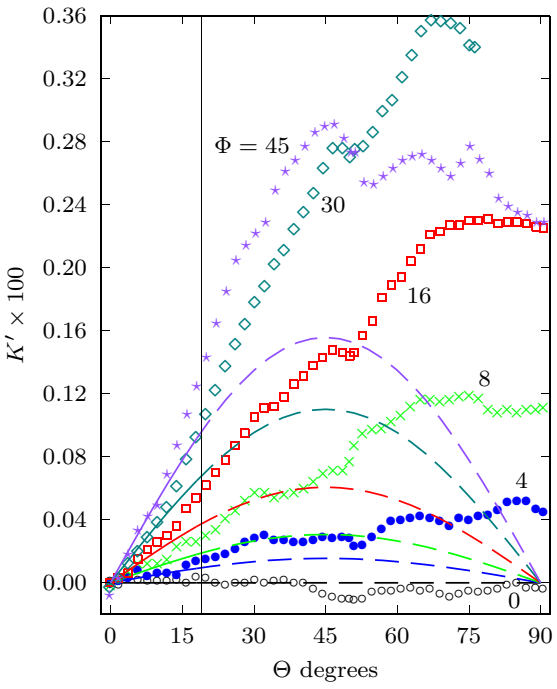

c) *Rolling moment versus incidence angle at various flow orientations. For clarity, the Φ = 60 and 75 degree data are not shown — they collapse towards the 90 degree data in (b).*

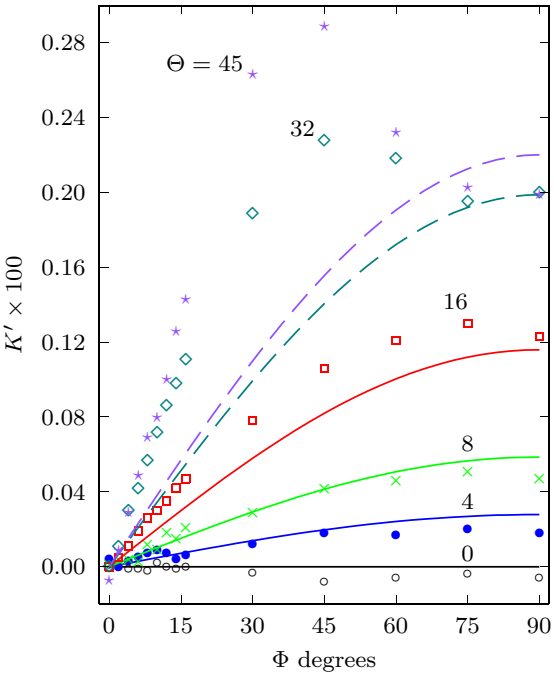

d) *Cross-plotting rolling moment versus flow orientation for various incidence angles.*

Figure 2 *The 1.5 m wind tunnel tests were flow incidence (Θ) sweeps from 0 to 90 degrees at fixed flow orientation (Φ) angles. The Mach number was 0.15. In (c) and (d), a tuned mass damper (TMD) was used to reduce vibration and the Reynolds number was 10 million.*

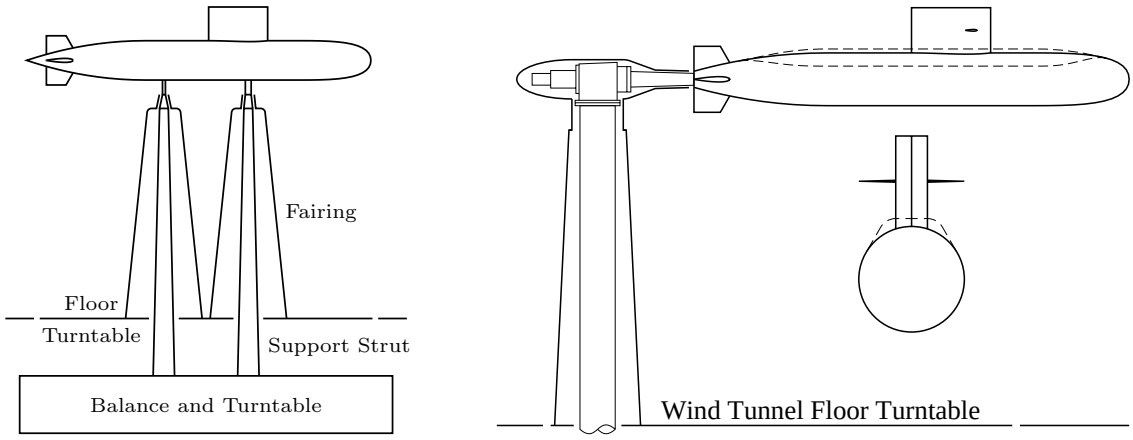

Figure 3 *Two Static Test Rig test configurations. With the two strut support, ±30 degree turntable (Θ) sweeps are conducted with the appendages fixed at various roll angles around the hull. With the sting support, 30 degree roll (Φ) sweeps are carried out at incidence.*

4 Static Test Rig High Incidence Roll Sweep Data

In the late 1980's and early 1990's, DREA and IAR implemented the Static Test Rig (STR) submarine model test capability in the IAR 9×9 m closed circuit atmospheric wind tunnel in Ottawa [14]. The STR (Figure 3) allows for steady state tests at incidence angles (Θ) up to 30 degrees at various flow orientations (Φ). Forces are measured on an external balance and extensive support strut tare and interference corrections can be made [15]. Flow field pressure and velocity measurements can be made using a flow survey rig.

This section presents STR data of relevance to the rising stability problem. The same model shape is tested as for the blowdown tunnel tests, with or without the sail, sailplanes, and/or deck. The model is 6 m long and is tested at wind speeds of 50 to 55 m/s giving Reynolds numbers of 20 to 23 million. Force measurements are corrected for tare and interference effects but flow field velocity measurements are not corrected.

The standard deviation in a STR rolling moment measurement is $100\sigma_{K'} \approx 0.001$. This accounts for balance resolution limits and a minor balance thermal drift problem. When tare and interference correction error is included, $100\sigma_{K'} \approx 0.003$. A thorough error analysis [16] that also examined geometry, dynamic pressure, blockage correction, support strut deflection correction, and other minor errors estimated the *upper bound* on K' error (the sum of the magnitudes of all the errors) at from 0.01×10^{-2} to 0.02×10^{-2}.

4.1 Hull Shadowing of Tail Appendages

The standard rolling moment equation (1) models the moment induced on the tail appendages by the wake from the hull in a crossflow [10]. This effect was investigated in STR roll sweep experiments with only the bare hull and symmetrical tail configuration (the 'HT' configuration; sail and deck are absent). The results, Figure 4, show that the effect is not measurable on this shape, unless the tailplanes stall.

Tailplane stall is possible in tight horizontal plane turns where yaw rotation results in the crossflow increasing in strength towards the tail. For a controlled, incidence limited rising maneuver, tailplane stall should not occur.

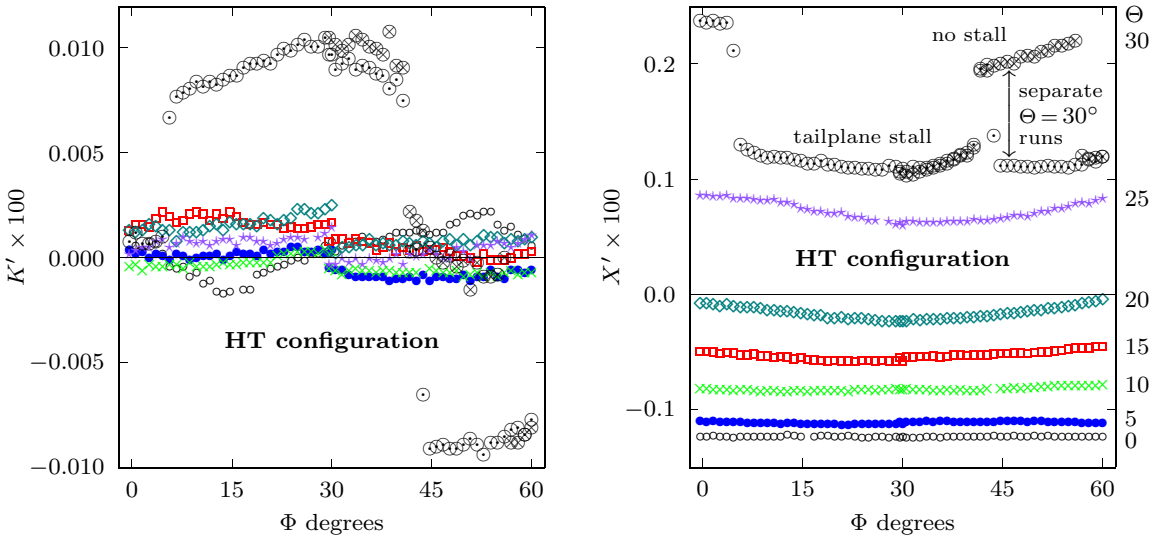

Figure 4 *STR roll sweep data for the axisymmetric hull and symmetrical tail configuration. For this configuration only, tare and interference corrections are not made to rolling moment, which is effectively zero. The moment is appreciable only when the tailplanes stall at $\Theta = 30$ degrees. Stall is detected by the sudden increase in drag (decrease in axial force X).*

4.2 Isolating the Trailing Sail Vorticity/Tail Interaction

Equation (1) models the unsteady hydrodynamics in a quasi-steady manner, by separating the moment into sail and tail contributions and allowing the tail moment to be a function of the crossflow at the sail $t = \tau_T$ seconds ago. These separate contributions are obtained by measuring the steady state rolling moment on the model with and without tail appendages. Such tests were done with the generic hull and sail (HS) and hull, sail, and tail (HST) configurations (the sailplanes and deck were absent) on the STR two strut support configuration. The data are presented in Figure 5.

The function that is least squares fitted to the rolling moment data in this paper is:

$$\begin{aligned} K'(\Theta,\Phi) = &\left(a_{11}\sin 2\Theta + a_{12}\sin^2\Theta + a_{13}\sin^3\Theta\right)\sin\Phi \\ &+ \left(a_{21}\sin 2\Theta + a_{22}\sin^2\Theta + a_{23}\sin^3\Theta\right)\sin 2\Phi. \end{aligned} \tag{3}$$

Powers of $\sin\Theta$ are used rather than mathematically conventional Fourier terms $\sin n\Theta$, $n = 1, 2, 3$ in order to simplify switching back to the usual state velocity formulation used in (1). Whether this or a Fourier series formulation is used, (3) has the advantage that it is easily extended to model as much detail as necessary throughout Θ, Φ space.

With $K'_{\rm HS}$ and $K'_{\rm HST}$ fitted with (3), the difference $K'_{\rm tail} = K'_{\rm HST} - K'_{\rm HS}$ giving the moment induced on the tail is easily calculated and is shown in Figure 6. The standard error in $K'_{\rm tail}$ is $\sigma = \sqrt{\sigma^2_{\rm HS} + \sigma^2_{\rm HST}} = 0.0032 \times 10^{-2}$.

$K'_{\rm tail}$ captures the strong nonlinearity that exists in the sail wake/tail interaction at incidence angles as low as 10 degrees. An explanation for the nonlinearity is suggested by the velocity measurements in Figure 6, taken at a yaw angle of 20 degrees [17]. At low incidence, the sail tip vortex image circulation is bound about the hull afterbody where it interacts approximately symmetrically with all the tail appendages to reduce the rolling moment. As incidence increases, the flow separates and a strong lower body separation vortex moves laterally away from the tail. This reduces the moment induced on the tail

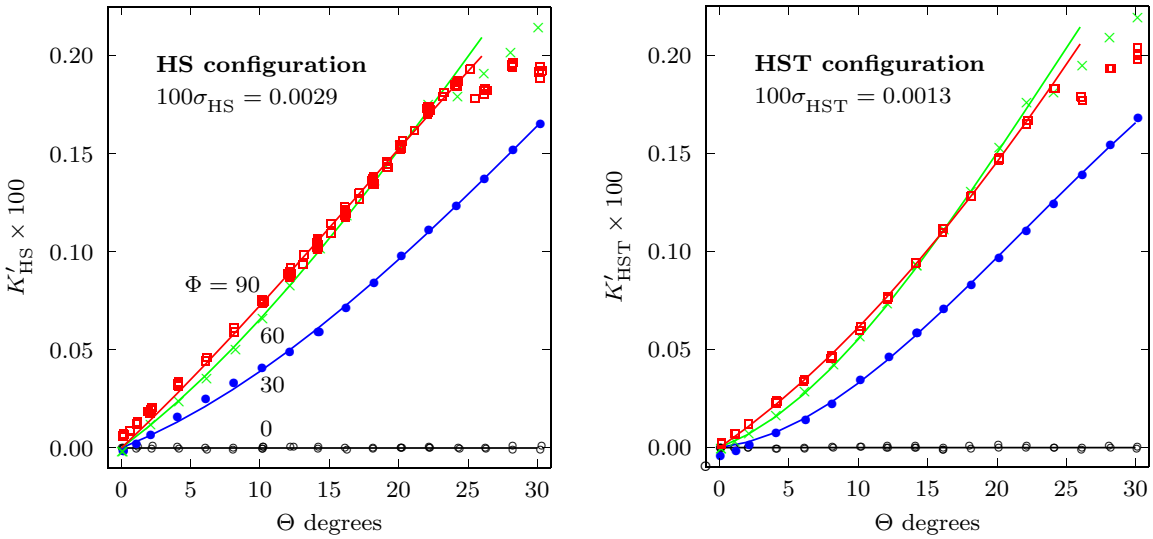

Figure 5 *STR two strut rolling moment incidence sweep data fitted with high order terms in Θ and Φ. The standard errors for the fits are indicated in each graph. For $\Phi = 60$ and 90 degrees, only the data below sail stall are fitted.*

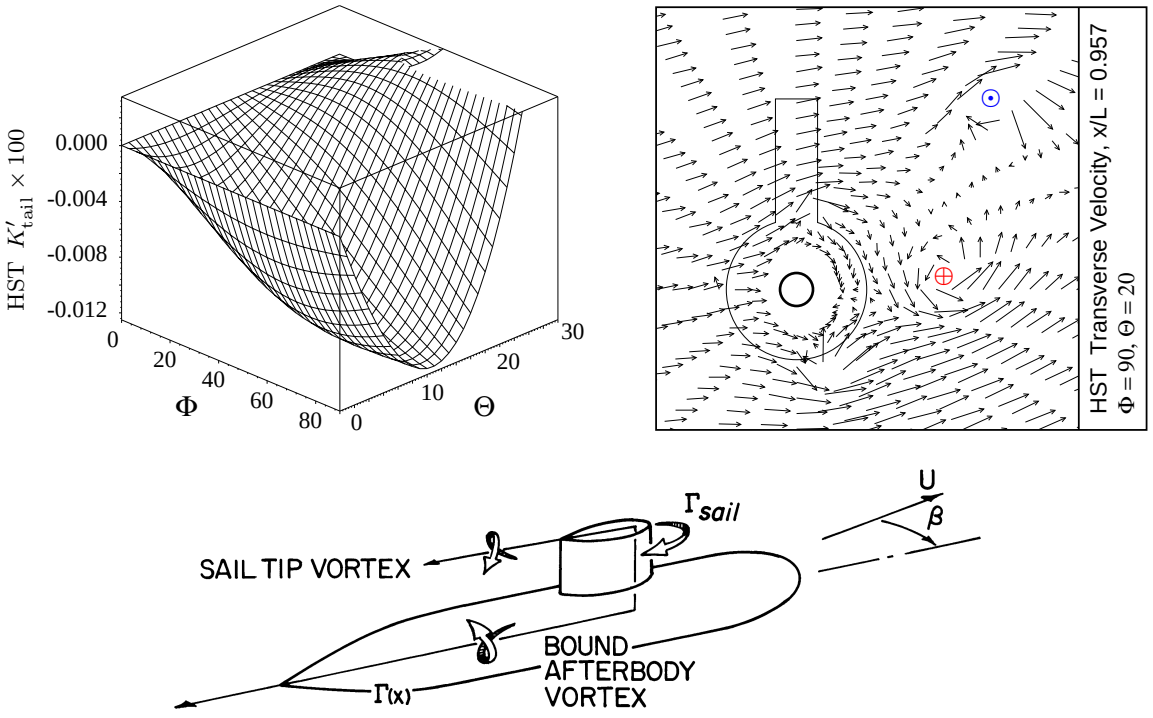

Figure 6 *The HST rolling moment generated at the tail (left) is highly nonlinear in Θ. This nonlinearity correlates with the hull bound vorticity (bottom) separating and moving away from the tail (right). The STR transverse velocity measurements on the right are taken in a transverse plane just aft of the tail. The local hull diameter is the heavy circle inside the submarine profile. The onset flow is from the left, the sail tip vortex is at $\odot$, and the lower body separation vortex at $\oplus$.*

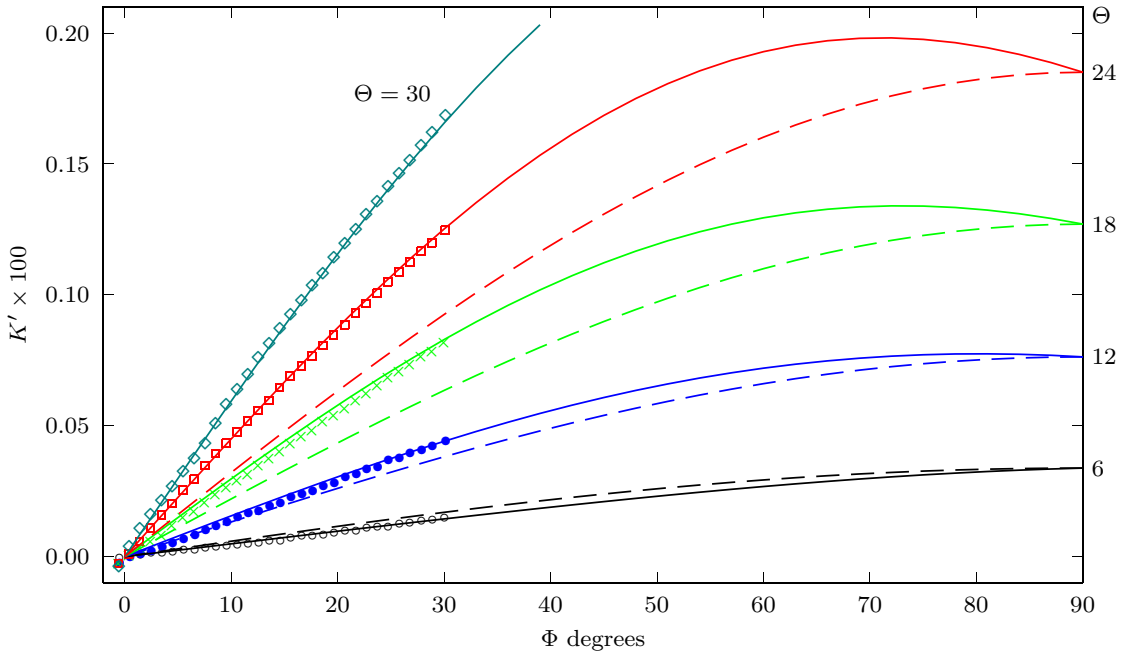

Figure 7 *HSST roll sweep data, the* $K'_{\text{HST}}(\Theta, \Phi)$ *function (solid lines), and standard* Φ *interpolation applied to the* $\Phi = 90$ *degree HST data:* $K'_{\text{HST}}(\Theta, 90)\sin\Phi$ *(dashed lines).*

and, at very high incidence when the lower body separation vortex interacts strongly with the starboard sternplane, actually increases the moment (K'_{tail} becomes positive).

The nonlinearity in K'_{tail} suggests that using the constant K'_i coefficient in (1) is incorrect beyond incidence angles at the tail of about 10 degrees.

4.3 Sailplane Effects and Φ Interpolation

Figure 7 shows STR rolling moment roll sweep data for the HSST model configuration (hull, sail, sailplanes, and tail) at the low Φ angles of interest for rising stability. These data agree well with the K'_{HST} fitting function showing that:

- the sailplanes do not have a large impact on rolling moment at low Φ angles, and
- the large 30 degree Φ increments in the HST incidence sweep data are fine enough that the interpolant (3) adequately models rolling moment from $\Phi = 0$ to 30 degrees.

Also shown in Figure 7 is the standard Φ interpolant applied to the $\Phi = 90$ degree incidence sweep data ($K'_{\text{HST}}(\Theta, 90)$). This model is good in the 0 to 12 degree Θ range but underpredicts $\partial K'/\partial\Phi$ by 20 to 30 percent for higher incidence angles.

4.4 HSSDT Tail and Deck Effects

Roll sweep data for the HSSDT configuration (generic model with sailplanes and deck, Figure 3) at low Φ angles are shown in Figure 8. Note the strong nonlinearity in Θ; that is, compare $\Delta K'_{\text{HSSDT}}$ as Θ changes from 2 to 4 degrees with that for Θ changing from 28 to 30 degrees (also see Figure 10 in the next section). High incidence rolling moment cannot be obtained by extrapolating from low incidence measurements.

The sail wake induced moment at the tail K'_{tail} is similar to that for the HST configuration (Figure 6), except at high Θ values.

The direct moment caused by the deck K'_{deck} has only a small linear variation in Θ so K'_{deck} is primarily from increased crossflow drag rather than lift. This is consistent with

a slender body theory view of the flow, where lift is purely a function of the maximum span of the lifting device (adding the deck does not increase the span of the sail). At lower test Reynolds numbers ($\mathbf{R} = 7$ million, see Mackay [18]), adding a deck has been shown to reduce the lift.

The lateral component of out-of-plane lift acting at $\bar{z}/\ell = -0.0043$ on the decked afterbody (the integral in (1)) is also included in the K'_{deck} function. This contribution has been independently estimated from the normal force on the hull in a pure yaw test as $100K'_{\text{out-of-plane}} = -0.036vw/U^2 = -0.018\sin^2\Theta\sin 2\Phi$, a function that looks remarkably like K'_{deck} in Figure 8 but with a negative peak amplitude at $\Theta = \Phi = 30$ degrees of -0.004. This contribution is quite small, as shown in Figure 9, and so it is not extracted from K'_{deck} for special treatment.

Figure 9 gives the relative contributions of the deck and tail components to rising stability as a function of incidence (variation with Φ is weak). While these contributions can be important at low incidence, they have only a small effect at the moderate incidence angles of interest to rising stability. In particular, the influence of the K'_{tail} term is less than 10% throughout the moderate to high incidence angle regime.

The error in:

$$\overline{\partial K_{\text{tail}}/\partial\Phi} = \left.\frac{\partial K_{\text{tail}}/\partial\Phi}{\partial K_{\text{HSSDT}}/\partial\Phi}\right|_{\Phi=0}$$

is also shown in Figure 9. It blows up as $\Theta, \Phi \to 0$ since $K_{\text{HSST}} \to 0$ here while its error remains constant.

5 Stability Analysis

This section assesses whether the underwater roll excursion of Figure 1 can be explained by the destabilizing hydrodynamic rolling moment overcoming the static stability as the speed of the boat steadily increases. The static stability is also known as the *metacentric* stability; its effect on the pitch stability of a submarine is evaluated by Hoyt and Imlay [19].

The following assumptions are made in the roll stability analysis of (1):

- The pitch (θ) and heading of the boat are constant, so $\dot{\theta}, q, r = 0$ and $p = \dot{\phi}$.
- The boat rolls slowly enough that second order terms in p can be neglected.
- The time lag in the induced hydrodynamic rolling moment at the tail is not modelled. The moment is small and so its effect will simply be bracketed by estimating stability with and without the tail being present.
- Minor asymmetrical trim effects, including propeller torque induced roll, are ignored. That is, $K'_*, f(\delta_r), Q_p, y_G, y_B = 0$.
- The submarine weight W is equal to its buoyancy B before the ballast tanks are blown. The center of gravity of the ballast water is assumed coincident with the hull centerline ($z = 0$), so after the complete evacuation of water from the blown tanks (which reduces W), $z_G W$ is unchanged. Thus, $z_G W - z_B B = \overline{BG}\, B$ in the analysis.
- The K'_{wp} coefficient, included in (1) because energy considerations require it [12,13], is replaced with $-K'_{\dot{v}}$, its exact equivalent in a potential flow.
- The rising maneuver takes place in a vertical plane, so $\Phi = \phi$ and:

$$\dot{v} - wp = \frac{d}{dt}\left(-u\tan\Theta\sin\phi\right) + u\tan\Theta\cos\phi\,\dot{\phi} = -\left(\dot{u}\tan\Theta + \frac{u\dot{\Theta}}{\cos^2\Theta}\right)\sin\phi \qquad (4)$$

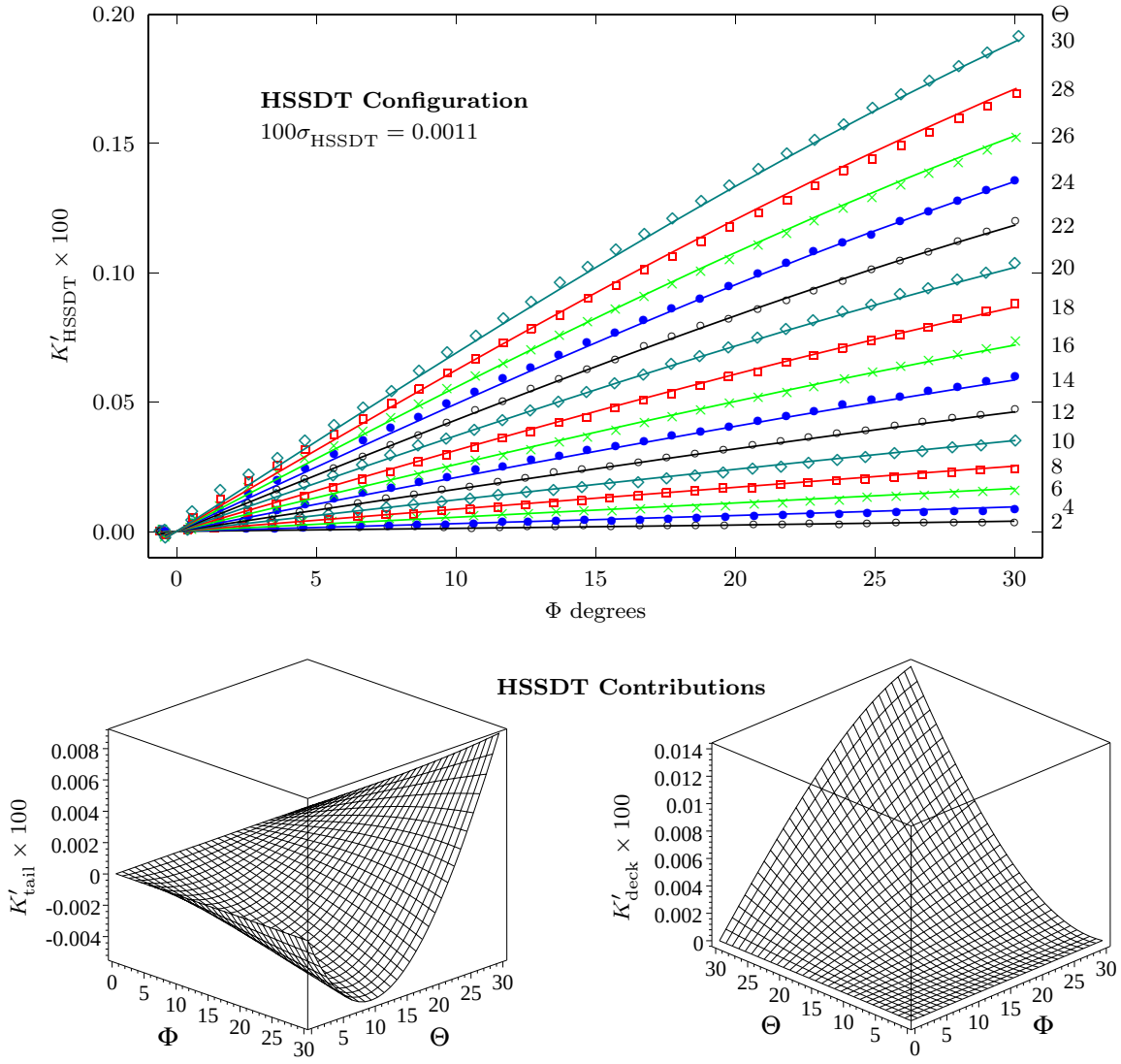

Figure 8 *The HSSDT roll sweep data and least squares fit (top). Subtracting HSSD from HSSDT data gives the induced moment on the tail* K'_{tail}. *Subtracting* K'_{HS} *from* K'_{HSSD} *gives the deck contribution* K'_{deck}, *ignoring the effect of the sailplanes. The standard errors are* $100\sigma_{\mathrm{tail}} = 0.0014$ *and* $100\sigma_{\mathrm{deck}} = 0.003$.

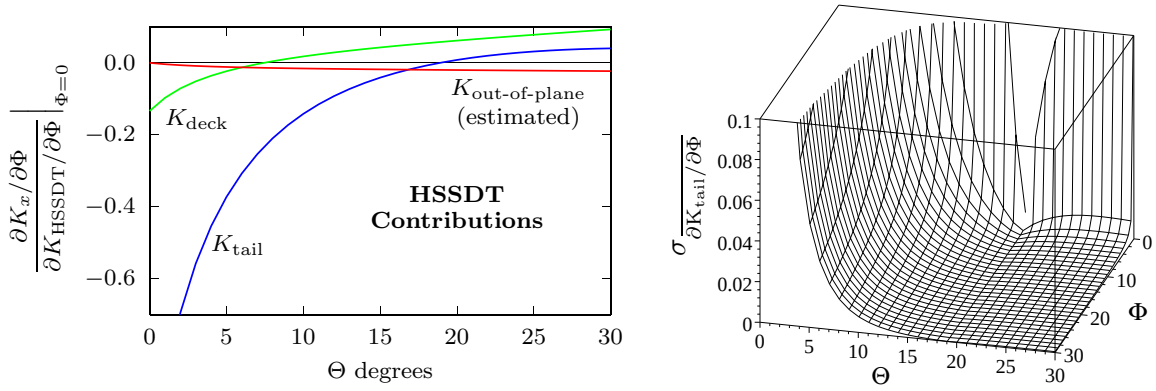

Figure 9 *The contributions to* $\partial K_{\mathrm{HSSDT}}/\partial\Phi$ *at* $\Phi = 0$, *and the error.*

Thus, (1) simplifies to:

$$\left(I_{xx} - K_{\dot{p}}\right)\ddot{\phi} - K_p u\dot{\phi} - \left(mz_G + K_{\dot{v}}\right)\left(\dot{v} - wp\right) = \frac{1}{2}\rho U^2 \ell^3 K'_{\mathrm{HSSD(T)}}(\Theta,\phi) - \overline{BG}\, B\cos\theta\sin\phi \tag{5}$$

where $K'_{\mathrm{HSSD(T)}}$ is given by (3) and represents either K'_{HSSD} or K'_{HSSDT}.

Hoyt and Imlay [19] and Booth [5,6] use classical linearized stability analysis, linearizing and simultaneously solving as many equations of motion as state variables they are considering. In (5), not only is $K'_{\mathrm{HSSD(T)}}$ proportional to the nonlinear product $\Theta\phi$ if it is independently linearized in Θ and ϕ, but it cannot be linearized in Θ and provide realistic solutions at high incidence angles. Therefore, a further assumption is made:

- Θ, u, and θ are decoupled from ϕ.

Figure 1 shows that this is approximately correct: Θ, u, and θ are relatively unaffected by an order of magnitude change in ϕ during the underwater roll excursion.

Treating Θ, u, and θ as just parameters in (5) and linearizing in ϕ gives an equation of the form:

$$a\ddot{\phi} + b\dot{\phi} + c\phi = 0 \qquad \text{with} \qquad a = I_{xx} - K_{\dot{p}}, \quad b = -K_p u. \tag{6}$$

Stability is determined by the solutions to (6) which are of the form $\phi \propto e^{st}$ with s a solution of the characteristic equation:

$$as^2 + bs + c = 0 \quad \Longrightarrow \quad s = \frac{-b}{2a} \pm \sqrt{\frac{b^2}{4a^2} - \frac{c}{a}}\,.$$

If $\Re(s) < 0$, then perturbations are damped out and the submarine is stable in roll; otherwise, perturbations grow and the submarine is unstable. Now, $I_{xx} > 0$, $K_{\dot{p}} < 0$, $K_p < 0$, and $u > 0$ always, so $-b/2a$ is always negative and the boat is stable if $c > 0$.

An examination of the $\dot{v} - wp$ term in (5), using (4) and state variable values from Figure 1, shows that it is two orders of magnitude less than the static stability term; therefore it is neglected. Finally then, the boat is stable at $\phi = 0$ if:

$$\frac{2V}{\ell^3}\frac{g\overline{BG}}{U^2}\cos\theta > \left.\frac{\partial K'_{\mathrm{HSSD(T)}}}{\partial\Phi}\right|_{\Phi=0} = R_{\mathrm{HSSD(T)}}(\Theta) \tag{7}$$

where:

$$R_{\mathrm{HSSD(T)}}(\Theta) = (a_{11} + 2a_{21})\sin 2\Theta + (a_{12} + 2a_{22})\sin^2\Theta + (a_{13} + 2a_{23})\sin^3\Theta. \tag{8}$$

Not surprisingly, stability is determined by the balance between the destabilizing hydrodynamic moment and the static righting moment. Figure 10 shows the two contributions to this balance, assuming it holds through the low ϕ angle regime. The hydrodynamic moment is overcome by the static moment at low speed and incidence angles only. At high incidence or speed, the hydrodynamic moment is strongest and the boat is vertically unstable. When

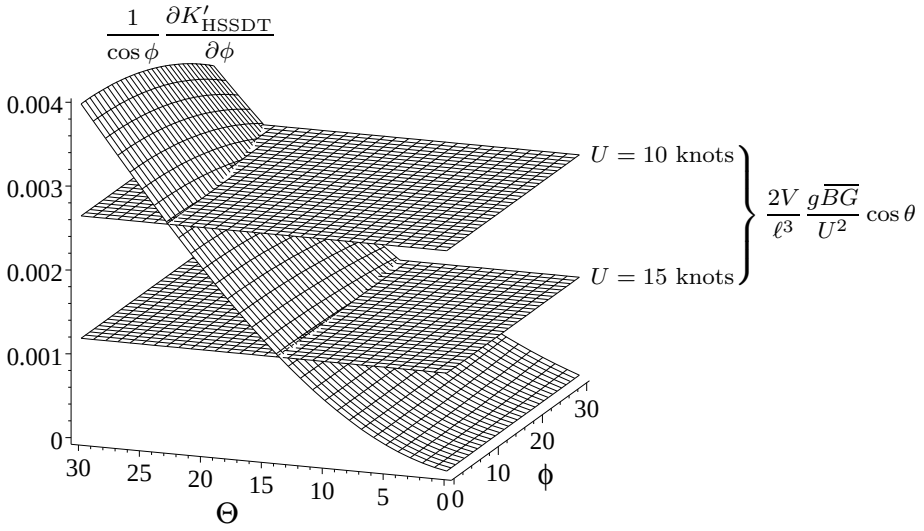

Figure 10 *The contributing terms to the stability balance:* $\partial/\partial\phi\big(RHS\ of\ (5)\big)\big/\cos\phi$. $\overline{BG} = 0.4$ *m,* $\theta = 15$ *degrees. Stability is insensitive to* θ *when it is small.*

stability is lost, it is lost almost simultaneously at all ϕ angles (it would be simultaneous but for the $\sin 2\Phi$ term in (3)), so that large roll excursions can occur suddenly.

Vertical stability is lost when the inequality in (7) breaks down, when:

$$u_c = \cos\Theta\sqrt{\frac{2V}{\ell^3}g\overline{BG}\cos\theta\Big/R_{\mathrm{HSSD(T)}}(\Theta)} \tag{9}$$

where the subscript c denotes the critical speed at the stability limit. Figure 11 shows this limit for a wide range of static stability levels. Also shown is the effect on stability of neglecting the contribution to rolling moment from the tail. The dashed lines are arguably the more correct stability limits since they represent the moment that can be immediately generated at the sail due to a small roll perturbation, before there is time for the vorticity generated at the sail to convect downstream and interact with the tail. However, the difference is small at moderate to large incidence angles.

Note that increasing speed or, to a much lesser extent, pitch angle reduces stability (see (7)). Yet increasing both these parameters are conventional strategies for reducing flow incidence, which is a way to increase stability. While further analysis is clearly required to determine an optimum strategy for avoiding instability, increasing pitch angle compromises stability the least and so is the preferred approach, at least when the boat is shallow. A pitch up attitude does result in buoyancy accelerating the boat forward, and if the boat is deep there is then time for the speed to build up, as in Figure 1. Of course, the two most straightforward ways to avoid instability are to reduce the ascent buoyancy and/or increase $\overline{BG}$. One way to increase $\overline{BG}$ is to blow the sail along with the ballast tanks; this would also substantially reduce the temporary instability on surfacing.

Booth's analyses [5,6] evaluate stability simultaneously in either three (v, p, r) or two (v, p) degrees of freedom, for an arbitrary value of w. The present analysis uses the transformation (2) and assumes Θ is constant to eliminate the need to consider v as an independent variable; at the same time, this allows arbitrarily large v or w magnitudes since the linearization is only in ϕ. This, in combination with better hydrodynamics modelling, improves the predictions considerably.

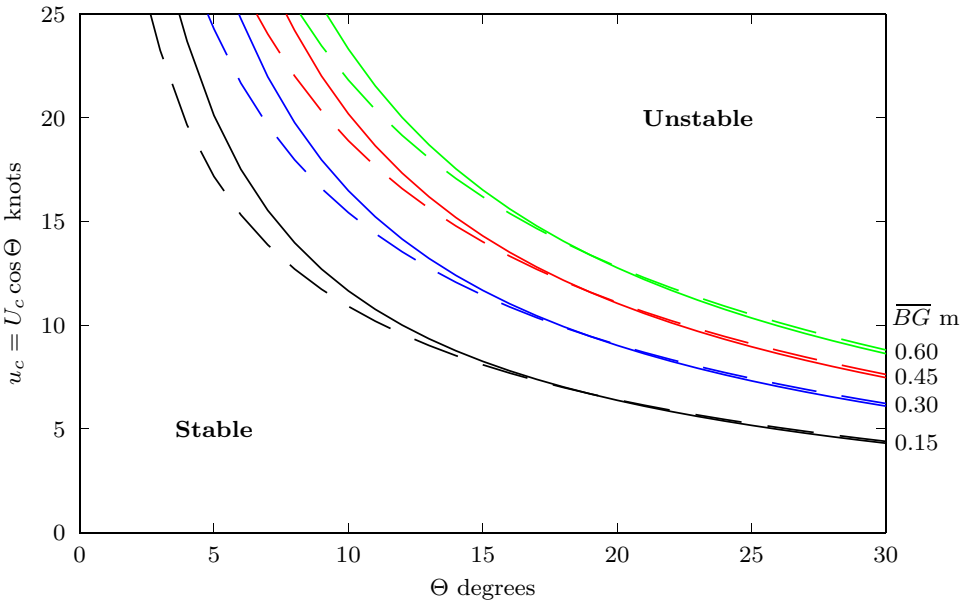

Figure 11 *Axial velocity at which analysis predicts roll stability is lost, assuming $\theta = 15$ degrees. The solid lines use R_{HSSDT} in (9) and the dashed lines use R_{HSSD}.*

Nevertheless, the stability limit (9) still does not adequately predict the underwater roll instability in Figure 1. This instability occurs early, at about 3/4 of the predicted stability limit for either velocity or flow incidence angle, assuming the $\overline{BG}$ value is correct. Alternatively, if the hydrodynamics modelling is correct, then the effective $\overline{BG}$ magnitude in the Figure 1 maneuver is only 60% of what it is thought to be. This is consistent with the findings of Hooft [3] and Bohlmann [4].

6 Concluding Remarks

Conventional captive model test regimes and hydrodynamic models underpredict the rolling moment on a submarine in a rising maneuver at moderate to high incidence angles. Captive model testing should take place at the flow orientations experienced by the maneuver being simulated. Hydrodynamic models require enough degrees of freedom to capture the nonlinearity.

Submarines are subject to an underwater roll instability caused by the destabilizing hydrodynamic rolling moment on the sail (increasing with U^2) overcoming the static righting moment (constant, independent of U) as the boat is accelerated upwards by buoyancy. However, a quasi-steady instability analysis, nonlinear in flow incidence, does not explain the early onset of instability in the case considered. Premature instability during rising maneuvers is not an isolated phenomenon and so further work is required to better model the physics of this maneuver.

Acknowledgment

This work was a collaborative effort with Dr. Jan Hooft of the Maritime Research Institute Netherlands and the Institute for Aerospace Research.

References

1. B.G.J. Wichers Schreur, "The Motion of Buoyant Bodies," Ph.D. Thesis, Trinity College, Cambridge, September 1990.
2. T.W. Binion and E. Stanewsky, "Observed Reynolds Number Effects: Low Aspect Ratio Wings and Bodies," Reynolds Number Effects in Transonic Flow, AGARD–AG–303, December 1988.
3. J.P. Hooft, private communication, July 1992.
4. H.J. Bohlmann, private communication, April 1999.
5. T.B. Booth, "Stability of Buoyant Underwater Vehicles Part I: Predominantly Forward Motion," International Ship Building Progress, vol. 24, no. 279, November 1977.
6. T.B. Booth, "Stability of Buoyant Underwater Vehicles Part II: Near Vertical Ascent," International Ship Building Progress, vol. 24, no. 280, December 1977.
7. M. Gertler and G.R. Hagen, "Standard Equations of Motion for Submarine Simulation," Naval Ship Research and Development Center, Report 2510, June 1967.
8. J. Feldman, "DTNSRDC Revised Standard Submarine Equations of Motion," David Taylor Naval Ship Research and Development Center SPD–0393–09, June 1979.
9. J.P. Feldman, "State-of-the-Art for Predicting the Hydrodynamic Characteristics of Submarines," Proc. of the Symp. on Control Theory and Navy Applications, US Naval Post-Graduate School, Monterey, July 1975.
10. J. Feldman, "Discussion of Submarine Equations of Motion," DTNSRDC informal report, September 1987.
11. M.A. Abkowitz, "Stability and Motion Control of Ocean Vehicles," M.I.T. Press, 1969.
12. F.H. Imlay, "The Complete Expressions for 'Added Mass' of a Rigid Body Moving in an Ideal Fluid," David Taylor Model Basin, Report 1528, July 1961.
13. G.D. Watt, "Estimates for the Added Mass of a Multi-Component, Deeply Submerged Vehicle," DREA TM 88/213, October 1988.
14. G.D. Watt, B. Tanguay, and K.R. Cooper, "Submarine Hydrodynamics in the Wind Tunnel: The DREA Static Test Rig," Royal Institute of Naval Architects (RINA) Warship '91 International Symposium on Naval Submarines 3, paper 19, London, May 1991.
15. V.D. Nguyen, Y. Drolet, and G.D. Watt, "Interference of Various Support Strut Configurations in Wind Tunnel Tests on a Model Submarine," AIAA paper 95–0443, 33rd Aerospace Sciences Meeting and Exhibit, Reno, January 1995.
16. Rowan Williams Davies & Irwin Inc., private communication, March 1991.
17. R.H. Wickens and F. de Souza, Institute for Aerospace Research, private communication, July 1993.
18. M. Mackay, "Estimation of the Force Due to a Submarine Sail or Similar Appendage," Third Canadian Marine Hydrodynamics and Structures Conference, Halifax, August 1995.
19. E.D. Hoyt and F.H. Imlay, "The Influence of Metacentric Stability on the Dynamic Longitudinal Stability of a Submarine," David Taylor Model Basin Report C–158, October 1948.

Paper: 27
Author: Dr. Watt

Question by Mr. Cunningham: Do you use or have you considered some type of stability augmentation system to minimize the roll instability?

Answer: Most submarines do not have roll control; i.e., their sternplanes and bowplanes or sailplanes do not differentially deflect. Submariners are also reluctant to add systems, especially active systems, if a problem can be solved another way.

Question by Dr. Khalid: Have you considered using numerical simulations as a possible means of investigating this instability problem?

Answer: Not an unsteady numerical simulation, mainly because the analytical analysis, based on the steady-state forces, seems to have solved the problem. We do use CFD to predict the steady-state forces on submarines, and it would be worth using the experimental data presented here to validate a CFD calculation.